Green-function approach to transport phenomena in quantum pumps

Liliana Arrachea
Instituto de Biocomputación y Física de Sistemas Complejos, Universidad de Zaragoza, Corona de Aragón 42, (50009) Zaragoza, Spain

(Received 2 May 2005; revised manuscript received 14 July 2005; published 30 September 2005)

We present a general treatment based on nonequilibrium Green functions to study transport phenomena in systems described by tight-binding Hamiltonians coupled to reservoirs and with one or more time-periodic potentials. We apply this treatment to the study of transport phenomena in a double barrier structure with one and two ac potentials. Among other properties, we discuss the origin of the sign of the net current.

DOI: 10.1103/PhysRevB.72.125349 PACS number(s): 72.10.−d, 73.23.−b, 73.63.−b

I. INTRODUCTION

The impressive development in the technology of fabrication of small circuits, enabled the investigation of single electron transport induced by time-periodic fields.[1] In a recent experiment by Switkes *et al.*[2] charge transport through a quantum dot is induced by means of two time-periodic potentials with a phase lag. This has renewed the interest in the study of charge pumping in open quantum systems, motivating theoretical[3–9] and experimental activity.[10] Closely related phenomena are the photovoltaic effect[11–13] in mesoscopic junctions and charge driving in molecular ratchets.[14,15] The main feature characterizing these effects is the generation of a net current as a response to a time-dependent external field without a net static bias.

Several theoretical treatments on quantum pumps rely on adiabatic approximations,[3–6] relevant for very slow potential modulations. A good amount of work on time-dependent transport is based on Floquet theory,[7–9,14–17] the scattering matrix approach[3,6,18] and the transfer matrix technique.[19] An alternative framework to investigate transport phenomena in mesoscopic devices and nanostructures is the description of the device in terms of tight-binding Hamiltonians and the solution of the problem with nonequilibrium Green functions. Since the proposals of Refs. 20 and 21, this kind of approach became widely extended in the study of electronic transport through a nanometric or mesoscopic sample, as a response to a static bias. One of the reasons for the success of this scheme is the fact that it is suited to deal with arbitrary high bias, finite temperature, arbitrary strength of dissipation and that it can be extended to include many-body interactions at least pertubatively. Another appealing feature of this approach is the possibility of combining it with the so-called *ab initio* methods to describe details of the contacts and molecular bridges of the devices.[22] In the context of transport problems with time-dependent fields, there are also basic proposals of this type of strategies[23,24] but, in comparison, not so many recent developments. Some examples are studies on ac-driven quantum dots and superlattices,[25–28] the latter restricted to weakly coupled quantum wells, studies on the dynamical Franz-Keldysh effect,[29] superconducting point contacts with a time-dependent voltage,[30] and conducting rings threaded by a time-dependent magnetic flux.[31–34] In these problems, the time-dependent part of the Hamiltonian is restricted to a single point,[25,26] a single bond[31–34] or to the contacts,[23,30] while approximations are introduced to deal with more general situations.[24,27–29]

In this work, we present a general treatment based on nonequilibrium Green functions to study transport phenomena in systems described by tight-binding models in contact with particle reservoirs with several time-periodic local potentials. We follow the main lines of Refs. 31 and 33 and we derive exact equations of motion for the Green functions. We present results on the transport properties in the special simple cases of one-dimensional systems with one and two time-dependent potentials. In the first case, some analytical expressions are available. In the second one, which is relevant for the experimental configuration of Ref. 2, we compute the Green functions numerically.

The traditional and intuitive way to think about stationary transport through a mesoscopic device placed between two electrodes at different chemical potentials is in terms of the behavior of the density of states of the central system and of its environment. In a time-dependent problem the density of states depends on time and its convolution with a Fermi function does not directly correspond to the notion of occupied energy states. In our study we analyze the connection between the transport behavior of the pumps, the density of states of the environment and the nonequilibrium spectral densities at the positions where the time-dependent potentials are applied.

In stationary transport like that resulting as the response to a static bias, the carriers responsible for the transport process are those injected from the electrodes with energies between the two different chemical potentials. A remarkable property of the pumping mechanism is that not only electrons with energies close to the Fermi energy of the reservoirs contribute to the net electronic current. Instead, *all* the electrons contribute to the net flow. This point has been previously addressed in Ref. 19 for the problem of an harmonically time-dependent potential in an asymmetric structure. We present here further details on this behavior which combines effects like photon-assisted tunneling, quantum interference and dissipation, sometimes giving rise to patterns that resemble a turbulent motion of electrons through the device.

The control of the direction of the net current is central for eventual technological applications of the pumping effect. However, the complex nature of the electronic motion generated in a quantum pump makes the prediction of this

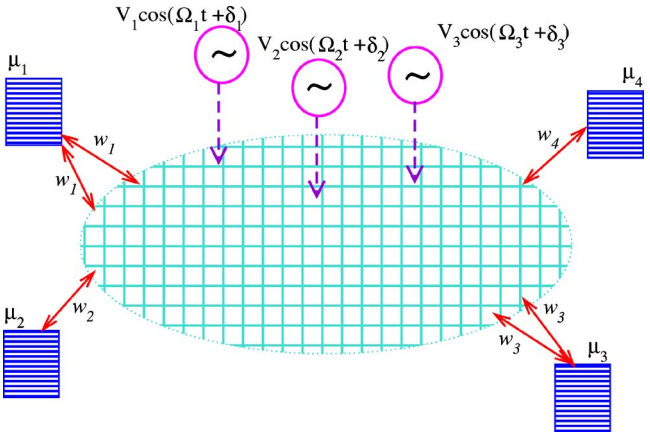

FIG. 1. (Color online) Scheme of the system described by Hamiltonian (1) with $L=4$ reservoirs and $M=3$ pumping potentials. The grid represents the sites of the central system and the boxes with stripes represent the reservoirs with chemical potentials μ_α, with $\alpha=1, \ldots, 4$.

property from *a priori* considerations a very difficult task. We discuss some operational conditions where the sign of the induced current can be understood and we also identify some mechanisms causing sign reversals. The paper is organized as follows. The theoretical treatment is presented in Sec. II. Examples and results are presented in Secs. III and IV. Finally, Sec. V is devoted to summary and conclusions.

II. THEORETICAL TREATMENT

A. General model and Green functions

We assume a general device, which consists in L reservoirs and a central system driven by several time-periodic local potentials. We do not include the effect of many-body interactions in our treatment. The full system is described by the Hamiltonian

$$H=\sum_{\alpha=1}^{L} H_\alpha-\sum_{\alpha=1}^{L} w_\alpha \sum_{k_\alpha,l_\alpha} a_{k_\alpha}^\dagger c_{l_\alpha}-\sum_{\langle lj\rangle} w_{lj} c_l^\dagger c_j+\sum_{l=1}^{N} \varepsilon_l c_l^\dagger c_l + \sum_{l=1}^{M} V_l \cos(\Omega_l t+\delta_l) c_{i_l}^\dagger c_{i_l}+\mathrm{H.c.}, \quad (1)$$

where the fermionic operators a_{k_α} denote degrees of freedom corresponding to the reservoir α, which is described by the Hamiltonian H_α. The contact of the reservoir α with the central region is represented by the hopping element w_α between the reservoir and the sites l_α placed at the boundaries of the lattice of the central system. The model for the latter piece is a tight-binding Hamiltonian with N lattice positions, hopping elements w_{lj} between pairs of sites $\langle lj\rangle$, and local energies ε_l. We also consider time-dependent potentials acting locally at M sites of the central system denoted by i_l, which oscillate with amplitudes V_l, frequencies $\Omega_l=n\Omega_0$ (being n an integer number) and phases δ_l. A scheme of the setup is shown in Fig. 1.

In what follows, we present a closed set of equations to calculate the Green functions corresponding to spacial coordinates of the central system. As usual,[35] we define retarded and lesser Green functions,

$$G_{l,m}^R(t,t')=-i\Theta(t-t')\langle\{c_l(t),c_m^\dagger(t')\}\rangle,$$

$$G_{l,m}^<(t,t')=i\langle c_m^\dagger(t')c_l(t)\rangle. \quad (2)$$

In the nonequilibrium formalism, Dyson equation for the Green function has a matricial structure which defines a coupled set of integro-differential equations for the lesser and retarded components. Following the standard procedure[20–24] we consider ideal noninteracting leads for the reservoirs. The corresponding degrees of freedom are integrated out, defining the self-energies,

$$\Sigma_{l,m}^{R,<}(t-t')=\delta_{l,l_\alpha}\delta_{m,l'_\alpha}|w_\alpha|^2\sum_{k_\alpha} g_{k_\alpha,k_\alpha}^{R,<}(t-t'), \quad (3)$$

which depend on the equilibrium Green functions $g_{k_\alpha,k_\alpha}^{R,<}(t-t')$ of the free reservoirs (i.e., isolated from the central system). The latter can be expressed in terms of densities of states $\rho_\alpha(\omega)$ through

$$\sum_{k_\alpha} g_{k_\alpha,k_\alpha}^R(t-t')=-i\Theta(t-t')\int_{-\infty}^{\infty}\frac{d\omega}{2\pi}e^{-i\omega(t-t')}\rho_\alpha(\omega),$$

$$\sum_{k_\alpha} g_{k_\alpha,k_\alpha}^<(t-t')=i\int_{-\infty}^{\infty}\frac{d\omega}{2\pi}e^{-i\omega(t-t')}f_\alpha(\omega)\rho_\alpha(\omega), \quad (4)$$

being $f_\alpha(\omega)=1/(e^{\beta(\omega-\mu_\alpha)}+1)$ the Fermi function.

We work in units where $\hbar=1$. The equations for the retarded and lesser components read

$$\left(-i\frac{\partial}{\partial t'}-\varepsilon_n-V_n(t')\right)G_{m,n}^R(t,t')-\sum_{l=1}^{N}G_{m,l}^R(t,t')w_{l,n}-\sum_{l=1}^{N}\int_{t'}^{t}dt_1 G_{m,l}^R(t,t_1)\Sigma_{l,n}^R(t_1-t')=\delta(t-t')\delta_{m,n},$$

$$\left(-i\frac{\partial}{\partial t'}-\varepsilon_n-V_n(t')\right)G_{m,n}^<(t,t')-\sum_{l=1}^{N}G_{m,l}^<(t,t')w_{l,n}-\sum_{l=1}^{M}\left(\int_{-\infty}^{t}dt_1 G_{m,l}^R(t,t_1)\Sigma_{l,n}^<(t_1-t')+\int_{-\infty}^{t'}dt_1 G_{m,l}^<(t,t_1)\Sigma_{l,n}^A(t_1-t')\right)=0, \quad (5)$$

being $V_n(t)=\delta_{n,i_l}V_l\cos(\Omega_l t+\delta_l), l=1,\ldots,M$.

We now present a very convenient way to calculate the Green functions. We start from the following integrated form of Eqs. (5):

$$G_{m,n}^<(t,t')=\sum_{i,j=1}^{N}\int_{-\infty}^{t}dt_1\int_{-\infty}^{t'}dt_2 G_{m,i}^R(t,t_1)\Sigma_{i,j}^<(t_1-t_2)G_{j,n}^A(t_2,t'),$$

$$G^R_{m,n}(t,t') = G^0_{m,n}(t-t') + \sum_{i=1}^{N} \int_{t'}^{t} dt_1 G^R_{m,i}(t,t_1) V_i(t_1) \times G^0_{i,n}(t_1-t'). \quad (6)$$

The advanced Green function is related to the retarded one through $G^A_{j,n}(t,t') = [G^R_{n,j}(t',t)]^*$. The equation for the lesser Green function is valid for long enough t,t', such that no memory on the initial condition is preserved. The "unperturbed" retarded Green function $G^0_{m,n}(t-t')$ corresponds to the solution of the problem of the central system *without* time-dependent potentials *coupled* to the reservoirs.

We now define the Fourier transform

$$G^R_{m,n}(t,\omega) = \int_{-\infty}^{t} dt' G^R_{m,n}(t,t') e^{i(\omega + i\eta)(t-t')}, \quad (7)$$

with $\eta = 0^+$, which leads to a linear set for the retarded Green function,

$$G^R_{m,n}(t,\omega) = G^0_{m,n}(\omega) + \sum_l \frac{V_l}{2} e^{i(\delta_l + \Omega_l t)} G^R_{m,i_l}(t,\omega-\Omega_l) G^0_{i_l,n}(\omega) + \sum_l \frac{V_l}{2} e^{-i(\delta_l + \Omega_l t)} G^R_{m,i_l}(t,\omega+\Omega_l) G^0_{i_l,n}(\omega). \quad (8)$$

In most of the cases, this set must be solved numerically, by discretizing ω introducing high and low frequency cutoffs $\pm K\Omega_0$, respectively. The parameter K depends on Ω_0 and must satisfy that $|K\Omega_0|$ is much larger than the absolute value of the highest frequency for which $G^0_{m,n}(\omega)$ has a finite spectral weight. In the numerical procedure, it must be checked that the solution of $G^R_{m,n}(t,\omega)$ does not depend on K.

Since $G^R_{m,n}(t,\omega)$ is a periodic function of t with period $\tau_0 = 2\pi/\Omega_0$, it is sometimes useful to work with the expansion,

$$G^R_{m,n}(t,\omega) = \sum_{k=-\infty}^{\infty} \mathcal{G}_{m,n}(k,\omega) e^{ik\Omega_0 t}, \quad (9)$$

being

$$\mathcal{G}_{m,n}(k,\omega) = \frac{1}{\tau_0} \int_0^{\tau_0} dt e^{-ik\Omega_0 t} G^R_{m,n}(t,\omega). \quad (10)$$

We stress that the advantage of writing the Dyson equation in the form (6) and working with the Fourier transform (7) is that the *exact* retarded Green function can be evaluated from a set of linear equations irrespectively the amount of time-periodic potentials. In addition, the present formulation in terms of Eq. (8) is very convenient to perform systematic expansions in powers of V_l.

B. Pumped current in a one-dimensional system coupled to two reservoirs

We now consider the case where the pumped system is a tight-binding chain with hopping elements between nearest neighbors, which is placed between left and right reservoirs. The Hamiltonian (1) reduces to

$$H = H_L + H_R + H_C(t) - w_L(a_L^\dagger c_1 + \text{H . c . }) - w_R(a_R^\dagger c_N + \text{H . c . }), \quad (11)$$

with $H_C(t)$ denoting the Hamiltonian for the central piece.

The current from the reservoirs to the central region can be written as

$$J_\alpha(t) = 2ew_\alpha \,\text{Re}[G^<_{i,\alpha}(t,t)], \quad (12)$$

with $\alpha = L$ and $i=1$ ($\alpha = R$ and $i=N$) for the current flowing from the left (right) reservoir. The dc components of the above currents are

$$J^{\text{dc}}_\alpha = \frac{1}{\tau_0} \int_0^{\tau_0} dt J_\alpha(t), \quad (13)$$

and due to the continuity condition, they satisfy $J^{\text{dc}}_L = -J^{\text{dc}}_R$ which allows us to write the dc J flowing through the central device as $J = (J^{\text{dc}}_L - J^{\text{dc}}_R)/2$.

Following Ref. 23 we write

$$J = \frac{1}{\tau_0} \int_0^{\tau_0} dt \int_{-\infty}^{t} dt_1 \,\text{Re}\{|w_L|^2 [G^R_{1,1}(t,t_1) g^<_L(t_1-t) + G^<_{1,1}(t,t_1) g^A_L(t_1-t)] - |w_R|^2 [G^R_{N,N}(t,t_1) g^<_R(t_1-t) + G^<_{N,N}(t,t_1) g^A_R(t_1-t)]\}. \quad (14)$$

Alternatively, it is also possible to calculate J from the dc component of the current flowing through an arbitrary bond $\langle l, l+1\rangle$ of the central tight-binding chain,

$$J_{l,l+1}(t) = 2ew_{l,l+1} \,\text{Re}[G^<_{l,l+1}(t,t)]. \quad (15)$$

Due to the continuity property, the dc component of (15) is independent of l and coincides with the result obtained from (14).

We consider zero temperature and the same chemical potential μ for the two reservoirs, hence $f_\alpha(\omega) = f(\omega) = \Theta(\mu - \omega)$. An interesting representation of J is found expressing it in terms of a *transmission* function $T(\omega)$,

$$J = e \int_{-\infty}^{\infty} d\omega f(\omega) T(\omega). \quad (16)$$

Evaluating $G^<_{l,l+1}(t,t)$ from (6) the explicit equation for the transmission function reads

$$T(\omega) = \frac{w_{l,l+1}}{\pi\tau_0} \int_0^{\tau_0} dt \{|w_L|^2 \rho_L(\omega) \text{Im}[G^R_{l,1}(t,\omega) G^A_{1,l+1}(\omega,t)] + |w_R|^2 \rho_R(\omega) \text{Im}[G^R_{l,N}(t,\omega) G^A_{N,l+1}(\omega,t)]\}. \quad (17)$$

The above representation of J exhibits a very important difference between the current generated in a quantum pump and the stationary transport caused by reservoirs at different potentials. In the latter situation, the current is expressed as $J = e\int d\omega T(\omega)[f_L(\omega) - f_R(\omega)]$. Namely, the spectral contribution of $T(\omega)$ to the net current corresponds to states with energies between the two different chemical potentials. Instead, in the pump *all* the states below the Fermi energy of the reservoirs contribute to the net current. Another important difference between these two kinds of transport mecha-

nisms is the origin of the direction of the current. In stationary transport, $T(\omega)$ is a positive-defined function, which is interpreted as the probability of tunneling, while the sign of J is determined by the bias represented by $f_L(\omega)-f_R(\omega)$. Instead, in time-dependent transport without static bias, the transmission function (17) can be either positive or negative and can also change sign as a function of ω. This function can be interpreted as the difference between the probability of tunneling from left to right and the probability of tunneling from right to left.

The next sections are devoted to evaluate explicitly $T(\omega)$ and J for the particular cases of one and two time-dependent potentials and to analyze in detail their behavior.

III. ONE HARMONICALLY TIME-DEPENDENT POTENTIAL

A. General considerations

The treatment exposed in the preceding section simplifies considerably for the case of only one ac potential ($M=1$). The Hamiltonian for the central system reads

$$H_C(t) = [V\cos(\Omega_0 t) - \varepsilon_1]c_1^\dagger c_1. \tag{18}$$

The reservoirs L and R are placed at the left and the right, respectively, of the pumping center, as explained in the preceding section. Our aim is the calculation of the net current. Using the expansion (9), the dc components of the currents flowing from the reservoirs towards the central site read

$$J_\alpha^{\mathrm{dc}} = e|w_\alpha|^2 \int_{-\infty}^{\infty} \frac{d\omega}{2\pi} f(\omega) \Big\{ -2\,\mathrm{Im}[\mathcal{G}_{1,1}(0,\omega)]\rho_\alpha(\omega) - \sum_k \rho_\alpha(\omega - k\Omega_0)\Gamma(\omega)|\mathcal{G}_{1,1}(k,\omega)|^2 \Big\}, \tag{19}$$

being $\Gamma(\omega)=|w_L|^2\rho_L(\omega)+|w_R|^2\rho_R(\omega)$. It is clear that a necessary condition for a nonvanishing J_α^{dc} is that the two terms of (19) do not cancel one another.

Further insight is gained by using the representation of the current in terms of the transmission function. In the present case, it is possible to solve recursively the set (8) to calculate the retarded Green function. This procedure is summarized in Appendix A. After replacing the expressions (A5) in (14), with $N\equiv 1$, it is found

$$T(\omega) = \frac{1}{\pi}|w_L|^2|w_R|^2 \sum_{k=-\infty}^{\infty} |\mathcal{G}_{1,1}(k,\omega)|^2 [\rho_L(\omega)\rho_R(\omega - k\Omega_0) - \rho_R(\omega)\rho_L(\omega - k\Omega_0)], \tag{20}$$

where it becomes clear that $J=0$ when (i) the system is symmetric under spacial inversion centered at the point where the pumping potential is applied, such that $\rho_L(\omega)=\rho_R(\omega)$, and (ii) the environment of the pumping point can be described by flat and approximately constant densities of states $\rho_\alpha(\omega)$. This expression for $T(\omega)$ resembles the mechanism of photon-assisted tunneling. The resulting equation for the current has a similar form as that obtained within the framework of the scattering matrix formalism, identifying the square of the scattering matrix in the Floquet formalism with the function $|\mathcal{G}_{1,1}(k,\omega)|^2\rho_L(\omega)\rho_R(\omega-k\Omega_0)$.[9] The current can be viewed as the result of processes where electrons leave the reservoir α with probability $\rho_\alpha(\omega)$, interact with the pumping center losing or gaining k energy quanta Ω_0 with probability $\propto|\mathcal{G}_{1,1}(k,\omega)|^2$, and exit to the opposite reservoir β with probability $\rho_\beta(\omega-k\Omega_0)$. The sign of the net current is completely determined by the structure of the functions $\rho_\alpha(\omega)$. Note that $T(\omega)$ may change sign as a function of ω. This means that electrons with different energies can flow in different directions and it is the sum of all these contributions that determines the sign of the net current.

For small Ω_0 and V, only a few modes k contribute. It is natural to associate such a situation with the idea of *adiabatic* pumping. More precisely, the concept of adiabatic pumping applies to the regime where the characteristic time scale for an electron to travel across the pump [proportional to the inverse of the width of the spectral peaks of $\mathcal{G}(k,\omega)$ as a function of ω] is much smaller than Ω_0. Adopting that definition, we see that it is possible in this case to have a finite J even in the adiabatic regime. The key is a high hybridization w_R, w_L of the pumping center with the environment, in order to allow for wide peaks in $\mathcal{G}(k,\omega)$, meaning a short life of the electrons at the pumping center. For low pumping frequencies and amplitudes, (20) can be expanded in powers of Ω_0 and it is found $T(\omega)\propto\Omega_0^2$.

A final interesting remark is that $J\propto|w_L|^2|w_R|^2$. This kind of behavior has already been found in molecular ratchets pumped by a laser field,[15] which are modeled on the basis of tight-binding Hamiltonians with asymmetric energy profiles and sincronic pumping centers.

B. Example

To illustrate the discussion of the preceding section we show some results of local pumping in a symmetric double barrier structure with the pumping potential acting at one of the barriers. The "unperturbed" structure has spacial inversion symmetry with respect to the center, which is broken by the effect of the time-dependent voltage.

A scheme of the device is shown in Fig. 2. For sake of clarity we write down the model Hamiltonian,

$$H = H_{\mathrm{leads}} + H_{\mathrm{cont}} - w\sum_{l=-N_L}^{0} c_l^\dagger c_{l+1} + Hc + \sum_{l=-N_L}^{1} \varepsilon_l c_l^\dagger c_l + V\cos(\Omega_0 t)c_1^\dagger c_1, \tag{21}$$

where ε_l defines the profile corresponding to the barriers. We consider a two-barrier structure of height E_b, $\varepsilon_{-N_L}=\varepsilon_l=E_b$ and $\varepsilon_l=0$, $l\neq -N_L,1$. We denote with H_{leads} the Hamiltonians of two semi-infinite chains which behave as macroscopic reservoirs and represent two external leads connected to the central device. These parts are pictorially represented by boxes with stripes in the scheme of Fig. 2 and we describe them by semicircular densities of states with bandwidth W,

$$\rho^0(\omega) = 4\sqrt{1-\omega^2/W^2}\,\Theta(W-\omega). \tag{22}$$

The term H_{cont} describes the hopping between the semi-infinite leads and the central structure and has the form of the

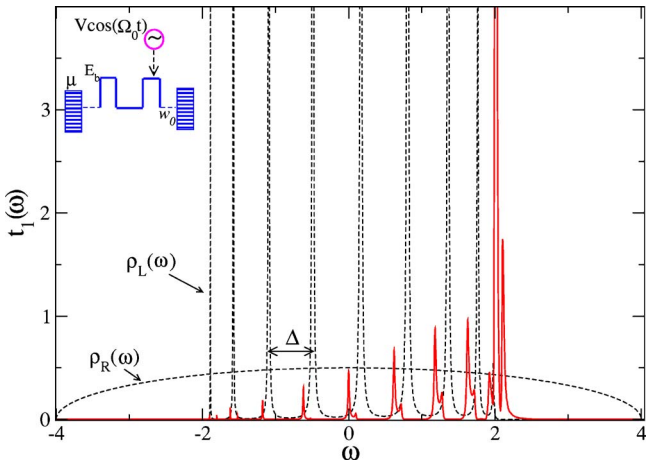

FIG. 2. (Color online) Solid (red) line, the function $t_1(\omega) = |\mathcal{G}(1,\omega)|^2$ for $V=0.1$, $\Omega_0=0.1$. Dashed (black) lines, the densities of states $\rho_L(\omega)$ and $\rho_R(\omega)$ of the left and right reservoirs, respectively. Δ denotes the energy difference between two consecutive energy levels in the double barrier structure. A scheme of the device is indicated in the upper left-hand corner. Other parameters are $E_b=1$, $|w_0|^2=0.1$, $W=4$, $N_L=9$.

last two terms of the Hamiltonian (11), with hopping parameter w_0.

In the notation of Eqs. (11) and (18), the right reservoir corresponds to the right lead, while the left reservoir corresponds to the left lead plus the double barrier structure with the exception of the point $l=1$, where the pumping voltage is applied. The ensuing degrees of freedom can be easily integrated out defining the following retarded Green functions for the left and right reservoirs:

$$g_L^R(\omega) = g^0(\omega) = \int_{-\infty}^{\infty} \frac{d\omega'}{2\pi} \frac{\rho^0(\omega')}{\omega - \omega' + i\eta}, \tag{23}$$

with $\eta=0^+$, and

$$g_R^R(\omega) = \cfrac{1}{\omega - \varepsilon_2 - \cfrac{w^2}{\omega - \varepsilon_3 - \ldots - \cfrac{w^2}{\omega - \varepsilon_{N_R} - w_0^2 g^0(\omega)}}}, \tag{24}$$

being the densities of states of the reservoirs $\rho_\alpha(\omega) = -2\,\mathrm{Im}[g_\alpha^R(\omega)]$. The hoppings between the pumping center and the left and right reservoirs are $w_L=w$ and $w_R=w_0$, respectively.

Figure 2 illustrates the behavior of the function $t_k(\omega) = |\mathcal{G}_{1,1}(k,\omega)|^2$, related to the probability for an incoming electron with energy ω to lose k energy quanta Ω_0 for selected parameters, along with the densities of states of the left and right reservoirs. All the energies are written in units of the hopping parameter w, which is set to $w=1$. All currents are expressed in units where $e=1$. The results shown in the figure correspond to a weak pumping amplitude ($V=0.1$), where only the contribution $k=1$ is sizable. For larger V, higher modes come also into play.

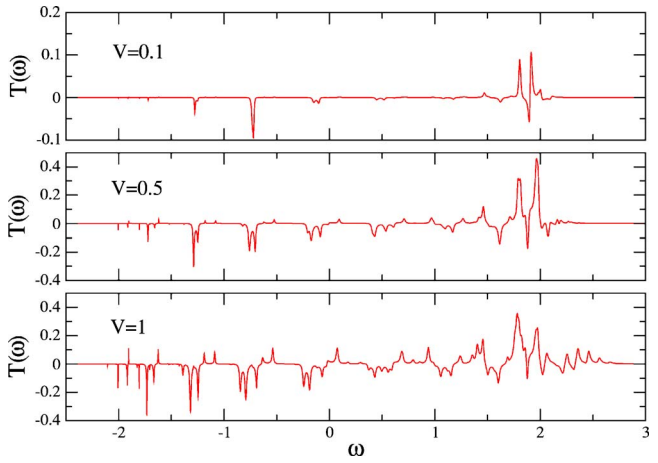

FIG. 3. (Color online) The transmission function $T(\omega)$ for $\Omega_0=0.1$ and $V=0.1,0.5,1$ (top to bottom). Other parameters are as in Fig. 2.

The resulting structure of the transmission function $T(\omega)$ is shown in Fig. 3 for a low frequency Ω_0 and different amplitudes V. The important feature to note is that for high ω and large pumping amplitude, this function can experiment with several changes of sign. This indicates that electrons with different energies may flow along different directions. The direction of the total dc being the cumulative sum of all these contributions.

Some results on the behavior of the net current J as a function of the chemical potential μ of the reservoirs are shown in Fig. 4. The structure of jumps and plateaus observed in the figure follows the patterns of resonances related

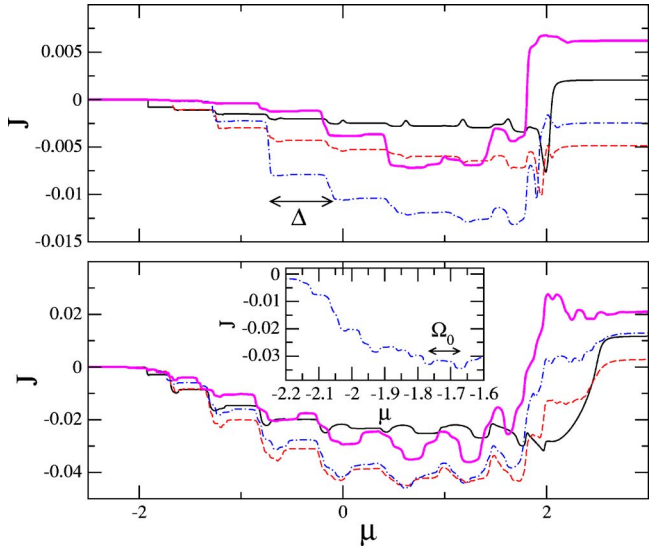

FIG. 4. (Color online) The dc J as a function of the chemical potential of the electrodes μ. Top and bottom panels corresponds to pumping voltages $V=0.2$ and $V=1$, respectively. Plots in thin solid (black), dashed (red), dotted-dashed (blue), and thick solid (magenta) lines correspond to $\Omega_0=0.01,0.05,0.1,0.2$, respectively. The spacing between two consecutive levels is indicated with Δ. The inset shows details for $V=2$ and $\Omega_0=0.1$. Other parameters are as in Fig. 2.

to the peaks of $t_k(\omega)$ and $\rho_L(\omega)$. The energy interval between two consecutive jumps in J is roughly the difference of energy between two energy levels Δ. For strong pumping amplitude, many k modes come into play in the transport process. The transmission function develops a richer structure where the spectral weight of the peaks associated to the free electronic levels split into several side peaks separated in $\sim\Omega_0$ (see bottom panel of Fig. 3). This is translated into peaks at the edges of the plateaus of J as a function of μ as shown in the bottom panel of Fig. 4. Details of the structure related to Ω_0 are shown in the inset.

For $\mu<2$, the chemical potential lies below the highest resonance of $\rho_L(\omega)$ and the behavior of $T(\omega)$ is consistent with a preference in the flow right to left, while for higher μ, the flow can take place in the opposite direction. Details depend on the frequency and amplitude of the pump, as well as on the degree of coupling between the double-barrier structure and the macroscopic reservoirs.

The behavior of the sign of J for $\mu<2$ is roughly the one expected from an intuitive adiabatic description, according to the following picture: during the part of the pumping cycle, where the potential decreases, the tunneling from the right macroscopic reservoir into the quantum well is favored, while during the remaining part of the cycle, the total potential at the right barrier increases and the electrons accumulated in the well are pushed from the right to the left. Remarkably, within this range of μ, the sign of J inferred from such a simple description remains unchanged for high Ω_0 and strong V, where such an adiabatic picture is not expected to be valid. The situation for higher μ is much less clear and strongly depends on the particular values of the pumping parameters.

To finalize, we want to remark that, due to the symmetry of the problem, the situation where the pumping potential is applied at the left barrier, would result in exactly the same behavior of J, but with the opposite sign. As discussed in the preceding section, a vanishing J would be obtained if the pumping potential were applied exactly at the center of the well between the two barriers.

IV. TWO HARMONICALLY TIME-DEPENDENT POTENTIALS IN A DOUBLE BARRIER STRUCTURE

A. General considerations

We now go back to Hamiltonian (11) and consider the following Hamiltonian for the central region,

$$H_C(t) = V\cos(\Omega_0 t+\delta)c_1^\dagger c_1 + \sum_{l=1}^{N}\varepsilon_l c_l^\dagger c_l - w\sum_{l=1}^{N}(c_l^\dagger c_{l+1}+\text{H.c.}) + V\cos(\Omega_0 t)c_N^\dagger c_N, \tag{25}$$

with the profile $\varepsilon_1=\varepsilon_N=E_b$, $\varepsilon_l=0$, $l=2,\ldots,N-1$, defining a double barrier structure. This arrangement is similar to the one of the experimental setup of Ref. 2, where two ac potentials with a phase-lag are applied at the walls confining a quantum dot.

In the interesting case of reservoirs with wide bands, it is possible to find an explicit relationship between the current and the local spectral functions at the points where the pumping potentials are applied. The wide band limit corresponds to approximately constant densities of states $\rho_\alpha(\omega)\sim\rho_\alpha$, such that

$$\int_{-\infty}^{t} G_{i,i}^{<}(t,t_1)g_\alpha^A(t_1-t) \sim iG_{i,i}^{<}(t,t)\rho_\alpha, \tag{26}$$

with $i=1$ for $\alpha=L$ and $i=N$ for $\alpha=R$. The expression (14) for the dc component of the current leads to

$$T(\omega) = |w_L|^2[\rho_L(\omega)[\rho_1^{\text{dc}}(\omega)-\bar{\rho}_1(\omega)] - |w_R|^2\rho_R(\omega)[\rho_N^{\text{dc}}(\omega) - \bar{\rho}_N(\omega)], \tag{27}$$

where we have defined the dc component of the generalized densities of states at the sites where the time-dependent potentials act,

$$\rho_i^{\text{dc}}(\omega) = -\frac{1}{\tau_0}\int_0^{\tau_0} dt 2\,\text{Im}[G_{i,i}^R(t,\omega)], \tag{28}$$

and the dc components of the spectral densities of occupation at those sites, $\bar{\rho}_i(\omega)$,

$$\bar{\rho}_i(\omega) = \frac{1}{\tau_0}\int_0^{\tau_0} dt\{|G_{i,1}^R(t,\omega)|^2|w_L|^2\rho_L(\omega) + |G_{i,N}^R(t,\omega)|^2|w_R|^2\rho_R(\omega),$$

$$n_i = -i\frac{1}{\tau_0}\int_0^{\tau_0} dt G_{i,i}^{<}(t,t) = \int\frac{d\omega}{2\pi}f(\omega)\bar{\rho}_i(\omega), \tag{29}$$

being n_i the density of particles at the site i. In an equilibrium system, these two spectral functions coincide, i.e., $\bar{\rho}_i(\omega)\equiv\rho_i^{\text{dc}}(\omega)$ and are positive defined functions, but in a time-dependent problem these two functions differ in general. While $\bar{\rho}_i(\omega)$ is a positive defined function, in a time-dependent problem $\rho_i(t,\omega)$ may change sign as a function of ω. Actually, it is clear from Eq. (27) that the violation of the equivalence between these two spectral functions, is at the heart of the existence of a nonvanishing dc. Another necessary condition is the breaking of left-right symmetry. This can be accomplished statically by, for example, considering $\rho_L(\omega)\neq\rho_R(\omega)$ or $w_L\neq w_R$, but also dynamically, by recourse to a finite phase lag $\delta\neq 0$ in the Hamiltonian (25). In what follows, we focus on the latter case.

B. Results

We consider the symmetric array of two barriers described in the preceding section, which are placed between two identical reservoirs with a large bandwidth $\rho_L(\omega)=\rho_R(\omega)=\rho^0(\omega)$ with the form defined in (22), and $|w_L|^2=|w_R|^2=|w_0|^2$. Due to the symmetry of the setup, $\rho_1^{\text{dc}}(\omega)=\rho_N^{\text{dc}}(\omega)$, while δ causes differences in the densities of occupation $\bar{\rho}_1(\omega)$ and $\bar{\rho}_N(\omega)$. In this way, the transmission function (27) simplifies to

$$T(\omega) = |w_0|^2\rho^0(\omega)[\bar{\rho}_N(\omega)-\bar{\rho}_1(\omega)], \tag{30}$$

and it is found that the current behaves like $J\propto(n_N-n_1)$. This is very suggestive, since it is natural to associate a difference

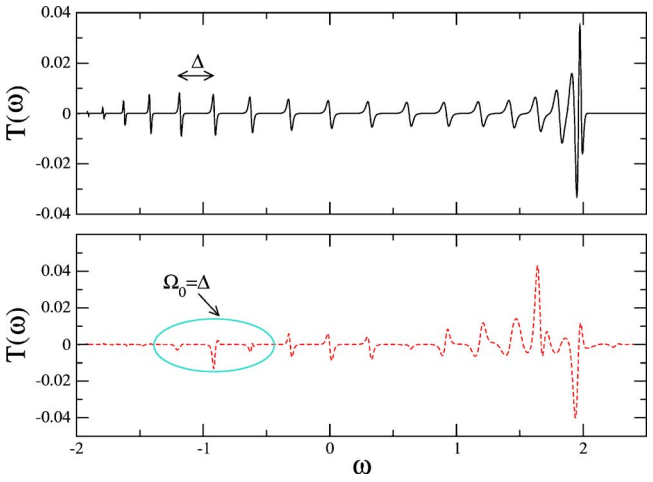

FIG. 5. (Color online) The transmission function $T(\omega)$ for a pumping amplitude $V=0.2$ a phase lag $\delta=\pi/2$ and frequencies $\Omega_0=0.01,0.3$ (top and bottom panels). The ellipse in the lower panel encloses a region where resonance is achieved. Other parameters are $E_b=1$, $|w_0|^2=0.5$, $W=4$, and $N=20$.

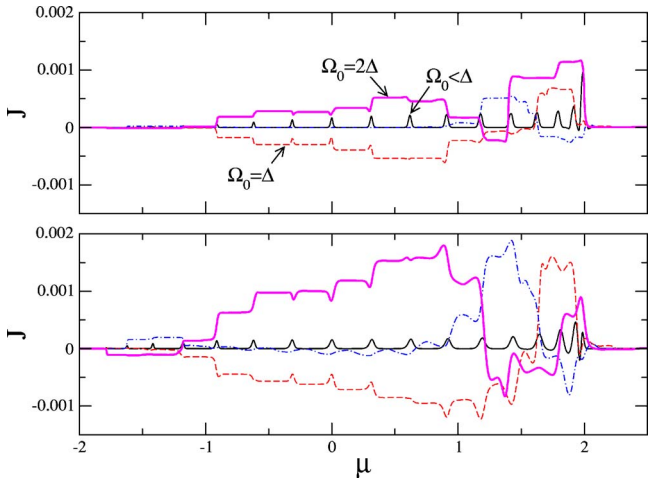

FIG. 6. (Color online) The dc J as a function of the chemical potential of the electrodes μ. Top and bottom panels corresponds to couplings to the macroscopic reservoirs $|w_0|^2=0.1$ and $|w_0|^2=0.5$, respectively. The pumping amplitude is $V=0.2$. Plots in thin solid (black), dashed (red), dotted-dashed (blue), and thick solid (magenta) lines correspond to $\Omega_0=0.01,0.3,0.45,0.6$, respectively. The spacing between two consecutive levels is referred to as Δ. Other parameters are as in Fig. 5.

in the local density of particles with a static potential drop. In the present case, we can imagine that the pumping with a phase lag induces an effective potential drop V_{eff} between the sites 1 and N, which causes a difference in the particle population at these two sites, and a current $J \propto V_{\text{eff}}$.

An important situation corresponds to the case of weak pumping amplitude V. A perturbative solution of the set (8) to the lowest order in V leads to

$$G^R_{m,n}(t,\omega) \sim G^0_{m,n}(\omega) + \frac{V}{2} e^{i(\delta+\Omega_0 t)} G^0_{m,1}(\omega-\Omega_0) G^0_{1,n}(\omega) + \frac{V}{2} e^{i\Omega_0 t} G^0_{m,N}(\omega-\Omega_0) G^0_{N,n}(\omega) + \frac{V}{2} e^{-i(\delta+\Omega_0 t)} G^0_{m,1}(\omega+\Omega_0) G^0_{1,n}(\omega) + \frac{V}{2} e^{-i\Omega_0 t} G^0_{m,N}(\omega+\Omega_0) G^0_{N,n}(\omega). \quad (31)$$

Using these expressions for the Green functions, making use of the fact that for the symmetric device $G^0_{11}(\omega)=G^0_{NN}(\omega)$ and $G^0_{1N}(\omega)=G^0_{N1}(\omega)$ and keeping terms to the lowest nonvanishing order in V, we find

$$T(\omega) \sim 2V^2|w_0|^4 \sin(\delta)[\rho^0(\omega)]^2 \,\text{Re}\{G^0_{11}(\omega)[G^0_{1N}(\omega)]^*\} \times \text{Im}\{G^0_{11}(\omega+\Omega_0)[G^0_{1N}(\omega+\Omega_0)]^* - G^0_{11}(\omega-\Omega_0) \times [G^0_{1N}(\omega-\Omega_0)]^*\}. \quad (32)$$

In order to have a better insight on the behavior of the function $T(\omega)$, we present some results in Fig. 5 for a phase lag $\delta=\pi/2$. In Fig. 5, we show the exact $T(\omega)$, calculated from Eq. (17). As the bandwidth of the macroscopic leads ($2W=8$) is large compared to the spectral width of the central piece (~ 4), the wide-band description for the reservoirs applies and we have checked that $T(\omega)$ is well reproduced by Eq. (30). The upper panel of Fig. 5 corresponds to small pumping amplitude V, small pumping frequency Ω_0 and $\delta=\pi/2$. The transmission function shows a peak-antipeak pattern with a separation Δ that coincides with the energy distance between two consecutive energy levels of the central structure. The peak-antipeak behavior of $T(\omega)$ indicates that, as the chemical potential increases and covers a level, electrons with lower energies within the linewidth are allowed to travel from the left to the right while the ones with higher energy travel in the opposite direction. The corresponding behavior of the dc component of the current as a function of μ is shown with thin (black) line in the upper panel of Fig. 6 and it consists in a succession of small peaks suggesting that as the chemical potential is increased covering an energy level of the central system, a conduction channel is enabled and a net current flows between the two reservoirs. The sign of the current is consistent with the one expected from intuitive considerations for this value of the phase lag on the basis of the following adiabatic picture: the first barrier lowers its effective potential during the part of the cycle where the second potential grows, favoring the incoming of electrons from the left reservoir inside the well. In the other part of the cycle, the voltage of the second barrier gets lower, helping the electrons to tunnel from the well towards the right reservoir.

An interesting situation takes place when the frequency is resonant, i.e., $\Omega_0=\Delta$. In this case, two neighboring electronic levels of the central device are expected to be mixed by the pumping potentials. The region marked in the lower panel of Fig. 5 satisfies the resonant condition and the function $T(\omega)$ consists of a sequence of antipeaks. The corresponding current is shown in dashed (red) lines in the upper panel of Fig. 6 and exhibits plateaus within this region. The sign corresponds to a net electronic flow from the right to the left

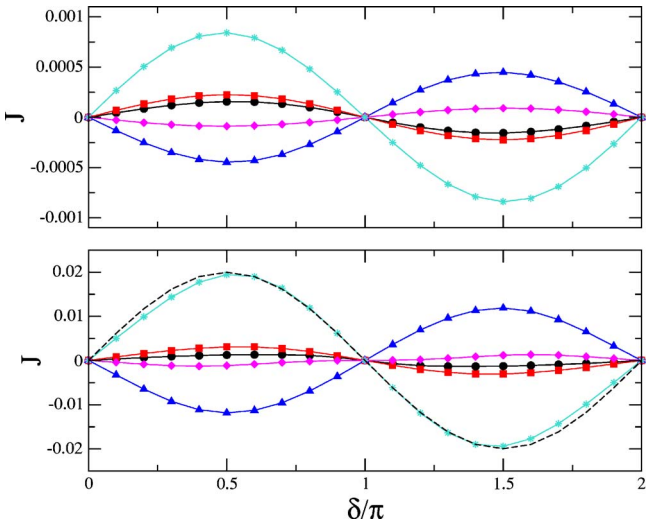

FIG. 7. (Color online) The dc J as a function of the phase lag δ for $\mu=0$ and $|w_0|^2=0.5$. Upper and lower panels correspond to pumping amplitudes $V=0.2$ and $V=1$, respectively. Circles, squares, triangles, diamonds, and stars correspond to $\Omega_0=0.01,0.05,0.3,0.45,0.6$, respectively. The function $J=0.0185\sin(\delta)$ is indicated in dashed lines in the lower panel. Other parameters are as in Fig. 5.

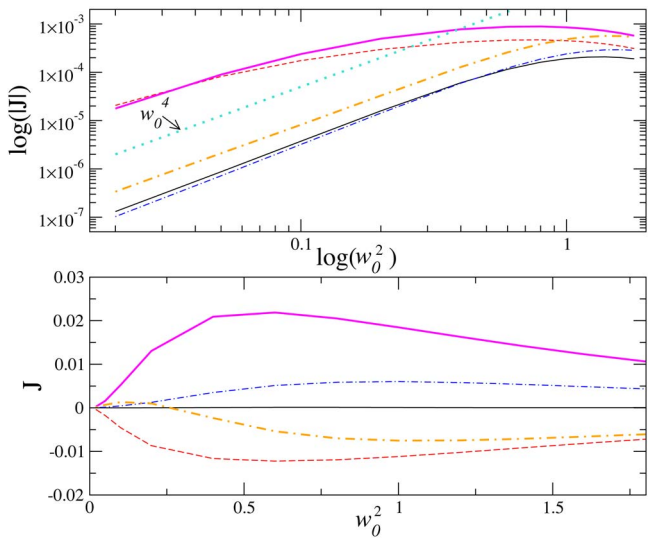

FIG. 8. (Color online) The dc J as a function of the contact parameter $|w_0|^2$ for $\delta=\pi/2$. The upper panel is plotted in log-log scale and corresponds to a pumping amplitude $V=0.2$ and chemical potential $\mu=0$. The reference slope corresponding to $J\propto|w_0|^4$ is plotted by the (light blue) dotted line. The lower panel corresponds to $\mu=1$ and pumping amplitude $V=1$. Plots in thin solid (black), dashed (red), dotted-dashed (blue), thick solid (magenta), and thick dashed-dotted (orange) lines correspond to $\Omega_0=0.1,0.3,0.45,0.6,0.75$, respectively. Other parameters are as in Fig. 5.

suggesting that the quantum interference due to the mixing of levels causes a sign reversal in comparison to the situation observed for pumping frequencies $\Omega_0<\Delta$. Also note in Fig. 6 that when the resonant condition is $\Omega_0=2\Delta$, the current recovers the sign of the situation $\Omega_0<\Delta$. For weak pumping amplitude V, a further examination on the origin of this interference is possible on the basis of the approximate solution given in Appendix B. The analysis presented there indicates that, at resonance, the effective phase lag between the two potentials is $\delta+j\pi$, being $j-1$ the number of energy levels of the structure between the two interfering ones. On the other hand, due to the symmetry of the problem, $J(\delta+j\pi)=(-1)^jJ(\delta)$, which complements the argument to explain why a shift in the phase lag may cause a change in the sign of the net current. The lower panel of Fig. 6 gives an idea of the effect of the changes in the linewidth of the central piece introduced through a stronger coupling to the reservoirs. As expected, these effects are more important at resonant frequencies since they help in the mixing of the electronic levels. For high energies, close to the upper edge of the spectrum ($\omega\sim2$), the energy levels are closer (Δ is smaller). Therefore, the resonant frequencies strongly differ from the ones at lower energies and sign reversals of J are observed as a function of μ.

The behavior of J as a function of the phase lag is shown in Fig. 7 for a selected value of the chemical potential μ. All the plots of the upper panel correspond to a small pumping amplitude and can be fitted by a function $\propto\sin(\delta)$, in full agreement with Eq. (32). The lower panel corresponds to a higher V and deviations from this behavior are found. For example, the plot in dashed lines corresponds to a function of the form $J=A\sin(\delta)$ and fits the behavior of J for $\Omega_0=0.6$ only in a neighborhood of $\delta=\pi$. Similar deviations are observed for other pumping frequencies.

The behavior of J as a function of the coupling to the reservoirs $|w_0|^2$ is shown in Fig. 8 for fixed μ, with different frequencies and pumping amplitudes. The higher panel corresponds to a low pumping amplitude and it is drawn in log-log scale in order to observe details for very low coupling to the reservoirs. In most of the cases, the current vanishes as the coupling to the reservoirs tends to zero following a law $J\propto|w_0|^4$ as suggested by (32). The corresponding reference slope is indicated in the figure for comparison. In some cases, slight deviations from this law are observed. One example is the plot in (red) dashed lines shown in the upper panel which corresponds to a resonant frequency. The origin for such departures should be found in the fact that the functions $G^0_{ij}(\omega)$ tend to be singular as the coupling to the reservoirs tends to vanish. The case of a larger pumping amplitude is illustrated in the lower panel of Fig. 8. A notable feature observed in the latter case is that changes in the strength of the coupling to the reservoirs may introduce changes in the sign of J, like in the case of the plot corresponding to $\Omega_0=0.75$. This is because the coupling to the reservoirs contributes to enhance the quantum interference between energy levels. For very small $|w_0|^2$, the behavior is similar to the one observed for weak V, illustrated in the higher panel.

Figure 9 shows J as a function of the pumping frequency Ω_0 for different values of the parameter $|w_0|^2$. The first feature to note is the structure of minima and maxima corresponding to resonant frequencies causing interference between nearest and next-nearest neighbor energy levels. The change of sign between resonances is consistent with the

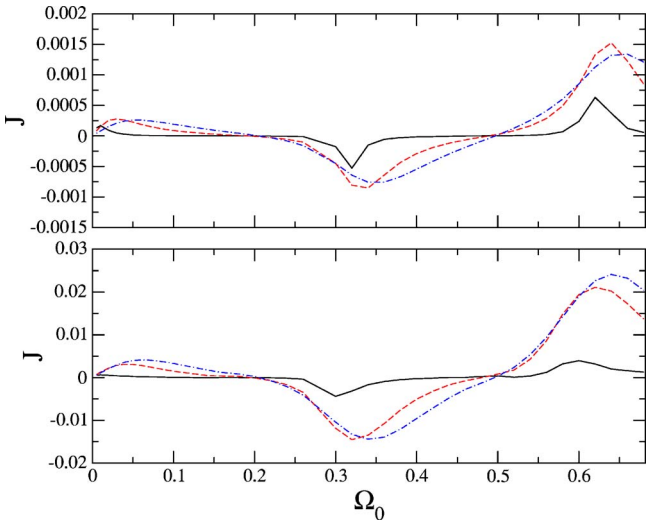

FIG. 9. (Color online) The dc J as a function of the pumping frequency Ω_0 for $\delta=\pi/2$, chemical potential $\mu=0$, and contact parameter $|w_0|^2=0.1,0.5,1$ [(black) solid, (red) dashed, and (blue) dotted-dashed lines]. Upper and lower panels correspond to pumping amplitudes $V=0.2$ and $V=1$, respectively. Other parameters are as in Fig. 5.

arguments of Appendix B and the discussion related to Figs. 5 and 6. Another issue worth mentioning is the linear behavior at very small pumping frequencies, as can be inferred from an expansion of the low V transmission function (32) in powers of Ω_0.

To finalize, we show in Fig. 10 the dc J as a function of the pumping amplitude V. For chemical potentials below the spectral edge, the behavior is consistent with $J \propto V^2$ within a rather wide range of V. This can be better observed in the log-log plot of the inset. This law is in agreement with the

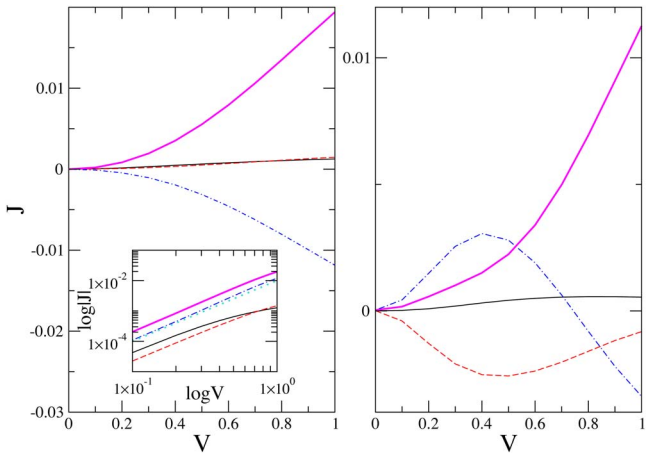

FIG. 10. (Color online) The dc J as a function of the pumping amplitude V for $\delta=\pi/2$ and $\Omega_0=0.01,0.1,0.3,0.6$ [(black) thin, (red) dashed, (blue) dotted-dashed, and (magenta) thick lines, respectively] and $|w_0|^2=0.5$. Left-hand and right-hand panels correspond to $\mu=0$ and $\mu=2$, respectively. The inset in the left-hand panel contains the same data of the main panel in log-log scale. The light blue dashed line indicates the slope for $J \propto V^2$. Other parameters are as in Fig. 5.

low V transmission function (32). Note that this behavior is followed at resonance within a wider range of V [see the plots in (blue) dotted-dashed and thick (magenta) lines in the left panel]. The right panel shows the situation for chemical potentials close to the spectral edge. In this case, the behavior for very small V remains in agreement with the law predicted by (32). For some pumping frequencies, however, J strongly deviates from this behavior at moderate V, in some cases showing sign reversals. Such dramatic changes have also been observed in molecular driven ratchets.[14,15] Their source must be found in the higher density of electronic levels at higher energy and the possibility of interference between more than two electronic levels as the pumping amplitude increases. As in the case of only one ac potential, the behavior of $T(\omega)$ within the high energy region has a much higher sensitivity to the particular values of parameters. Hence, the prediction of the sign of the current when the chemical potential tunes this spectral region becomes a much more difficult task.

V. SUMMARY AND CONCLUSIONS

We have presented a general approach based on nonequilibrium Green functions to study transport phenomena originated in time-periodic potentials applied on quantum systems described by tight-binding Hamiltonians without many-body interactions. The present treatment allows for the exact solution in problems with several time-dependent potentials provided that the oscillating frequencies are commensurate (i.e., a multiple of an elementary frequency Ω_0). In addition, the present treatment is valid for arbitrary amplitudes and oscillating frequencies of the time-dependent potentials.

We have employed the general treatment of Sec. II to study two simple problems of quantum pumping in a one-dimensional model for a double barrier structure connected to left and right reservoirs. We have first considered only one pump acting on one of the barriers. This case is interesting because an explicit analytical expression for the retarded Green function can be found. We have shown that the existence of a net electronic transport depends exclusively on the structure of the environment of the pumping center and two simple conditions must be fulfilled, the geometrical arrangement must not have spacial inversion symmetry with respect to the pumping center and it must have resonant levels.

The second case we have considered corresponds to pumping potentials oscillating with the same frequency and a phase-lag between them, acting at both of the barriers. This kind of operational arrangement of ac potentials is just the one used in the experiment of Ref. 2. In particular, we have shown that for weak pumping amplitude, the net current behaves like $J \propto \sin(\delta)$ as a function of the phase lag, in agreement with the experimental work. Another interesting feature is that for reservoirs with wide bands (as is often the case in double barrier structures in semiconductor junctions), the current can be related to the difference in the charge density at the pumping points.

We have stressed the fact that all electrons below the Fermi energy of the reservoirs contribute to the current generated by pumping mechanisms. We have also devoted some

effort to understand the conditions that determine the direction of the net current. We have found that in the two cases analyzed, this direction coincides with the one predicted by a "naive" adiabatic picture in the situations where quantum interference does not play a role. This condition seems to be more easily achieved in the case of only one pumping potential. Instead, for the case of two pumping potentials it is achieved for not too strong pumping amplitudes, when the pumping frequency is smaller than the separation between consecutive energy levels. For resonant frequencies, sign reversals take place due to quantum interference of different electronic levels. In both examples, there are regions close to the spectral edge where the transmission function experiments with many changes of signs. In this region, the details strongly depend on the parameters. We have also shown that the current behaves linearly in Ω_0 when the pumping frequency is small and proportional to V^2 for low pumping amplitudes. At resonance, the latter behavior extends to a range of V beyond the one expected from arguments based in perturbation theory.

The investigation of the pumping effect in systems with annular topology and the combination of the time-dependent effects with electron-electron, electron-phonon interactions and disorder is left to the future.

ACKNOWLEDGMENTS

The author thanks useful conversations with G. Chiappe, L. Martín-Moreno, S. Flach, S. Denysov, as well as the hospitality of Professor Fulde at the MPIPKS-Dresden, where part of this work has been done. Support from the Alexander von Humboldt Stiftung, PICT 03-11609 from Argentina, BFM2003-08532-C02-01 from MCEyC of Spain, grant "Grupo consolidado DGA" and from the MCEyC of Spain through "Ramon y Cajal" program are acknowledged. The author is a staff member of CONICET, Argentina. The numerical work was done at BIFI cluster.

APPENDIX A: EVALUATION OF THE RETARDED GREEN FUNCTION FOR A SINGLE HARMONICALLY TIME-DEPENDENT POTENTIAL

We present the solution of the set (8) for the case of only one periodic potential. In this case, it is possible to obtain an analytical expression for $G^R_{1,1}(t,\omega)$ through a recursive procedure. After some algebra, we find an expression with the structure (9), with the following coefficients:

$$\mathcal{G}_{1,1}(k,\omega) = \left(\frac{V}{2}\right)^k g^{\text{eff}}(\omega)\prod_{m=1}^{k} g^{(-m)}(\omega - m\Omega_0), \quad k>0$$

$$= \left(\frac{V}{2}\right)^{-k} g^{\text{eff}}(\omega)\prod_{m=1}^{-k} g^{(m)}(\omega + m\Omega_0), \quad k<0,$$

$$\mathcal{G}_{1,1}(0,\omega) = g^{\text{eff}}(\omega), \tag{A1}$$

where

$$g^{\text{eff}}(\omega) = \frac{1}{\omega - \varepsilon_1 - \sum^{\text{eff}}(\omega)},$$

$$\sum^{\text{eff}}(\omega) = \sum^{0}(\omega) + \left(\frac{V}{2}\right)^2 [g^{(1)}(\omega+\Omega_0) + g^{(-1)}(\omega-\Omega_0)]. \tag{A2}$$

The "bare" self-energy $\Sigma^0(\omega) = |w_L|^2 g^R_L(\omega) + |w_R|^2 g^R_R(\omega)$ represents the environment and is completely defined from the free Green functions of the pieces at the left (L) and at the right (R) of the pumping center. The function $g^{(m)}(\omega + m\Omega_0)$ can be expressed as a continued fraction defined from the recursion relation

$$[g^{(m)}(\omega + m\Omega_0)]^{-1} = \omega + m\Omega_0 - \varepsilon_1 - \sum^{0}(\omega + m\Omega_0) - \left(\frac{V}{2}\right)^2 g^{(m\pm1)}[\omega + (m\pm1)\Omega_0], \tag{A3}$$

where $+,-$ corresponds to $m>0$ and $m<0$, respectively. In practice, a cutoff is introduced such that $g^{(\pm K)}(\omega \pm K\Omega_0) = [\omega \pm K\Omega_0 - \Sigma^0(\omega \pm K\Omega_0)]^{-1}$, being K large enough in order to satisfy that $|K\Omega_0|$ is much larger than the absolute value of the energy for which the bare Green function $[\omega - \Sigma^0(\omega)]^{-1}$ has nonvanishing spectral weight.

Using the fact that

$$\text{Im}[\mathcal{G}_{1,1}(0,\omega)] = -\,\text{Im}\left[\sum^{\text{eff}}(\omega)\right]|g^{\text{eff}}(\omega)|^2, \tag{A4}$$

and the definition of $\Sigma^{\text{eff}}(\omega)$, we find

$$\text{Im}[\mathcal{G}_{1,1}(0,\omega)] = -\sum_k \text{Im}\left[\sum^{0}(\omega - k\Omega_0)\right]|\mathcal{G}_{1,1}(k,\omega)|^2. \tag{A5}$$

APPENDIX B: APPROXIMATE SOLUTION FOR THE RETARDED GREEN FUNCTION FOR TWO HARMONIC POTENTIALS AT RESONANCE

Let us start by noting that the retarded Green function for a tight-binding chain with hopping w and length N with open boundary conditions at both ends is

$$g^R_{lm}(\omega) = \sum_k \frac{\sin(kl)\sin(km)}{\omega - \epsilon_k + i\eta}, \tag{B1}$$

being $\eta = 0^+$, $\epsilon_k = -w\cos(k)$, and $k = n\pi/(N+1)$, with $n = 1,\ldots,N$.

We assume that the resonant energies ϵ_k and phases of the wave function of the double barrier structure connected to the reservoirs are approximately those of an open tight-binding chain of the same length and we propose the following ansatz for the retarded Green function evaluated at a resonant frequency ϵ_k,

$$G^0_{lm}(\epsilon_k) \sim \gamma_k \sin(kl)\sin(km). \tag{B2}$$

We have verified that this ansatz reproduces with reasonable accuracy the phases of the Green function in the present

model when the coupling to the reservoirs is not too weak.

Let us consider weak pumping amplitude and a pumping frequency such that $\Omega_0=\epsilon_{k_1}-\epsilon_{k_2}$, being $k_1-k_2=j\pi/(N+1)$ being j a positive integer. The set (31) reduces to

$$G^R_{m,n}(t,\epsilon_{k_1}) \sim G^0_{m,n}(\epsilon_{k_1}) + \frac{V}{2}e^{i(\delta+\Omega_0 t)}G^0_{m,1}(\epsilon_{k_2})G^0_{1,n}(\epsilon_{k_1}) + \frac{V}{2}e^{i\Omega_0 t}G^0_{m,N}(\epsilon_{k_2})G^0_{N,n}(\epsilon_{k_1}),$$

$$G^R_{m,n}(t,\epsilon_{k_2}) \sim G^0_{m,n}(\epsilon_{k_2}) + \frac{V}{2}e^{-i(\delta+\Omega_0 t)}G^0_{m,1}(\epsilon_{k_1})G^0_{1,n}(\epsilon_{k_2}) + \frac{V}{2}e^{-i\Omega_0 t}G^0_{m,N}(\epsilon_{k_1})G^0_{N,n}(\epsilon_{k_2}). \quad \text{(B3)}$$

The replacement of the ansatz (B2) in the above equations reveals that there is a phase equal to $j\pi$ between the terms proportional to $Ve^{\pm i(\delta+\Omega_0 t)}$ in relation to the ones proportional to $Ve^{\pm i\Omega_0 t}$ in the above expressions for $G^R_{m,n}(t,\epsilon_{k_i})$. This indicates that the effective phase lag between the two potentials is $\delta+j\pi$.

[1] L. J. Geerligs, V. F. Anderegg, P. A. M. Holweg, J. E. Mooij, H. Pothier, D. Esteve, C. Urbina, and M. H. Devoret, Phys. Rev. Lett. **64**, 2691 (1990).
[2] M. Switkes, C. M. Marcus, K. Campman, and A. C. Gossard, Science **293**, 1905 (1999).
[3] P. W. Brouwer, Phys. Rev. B **58**, R10135 (1998).
[4] F. Zhou, B. Spivak, and B. Altshuler, Phys. Rev. Lett. **82**, 608 (1999).
[5] T. A. Shutenko, I. L. Aleiner, and B. L. Altshuler, Phys. Rev. B **61**, 10366 (2000).
[6] O. Entin-Wohlman, A. Aharony, and Y. Levinson, Phys. Rev. B **65**, 195411 (2002).
[7] M. Moskalets and M. Büttiker, Phys. Rev. B **70**, 245305 (2004).
[8] M. Moskalets and M. Büttiker, Phys. Rev. B **69**, 205316 (2004).
[9] M. Moskalets and M. Büttiker, Phys. Rev. B **66**, 205320 (2002).
[10] L. DiCarlo, C. M. Marcus, and J. S. Harris, Phys. Rev. Lett. **91**, 246804 (2003).
[11] C. T. Liu, J. M. Liu, P. A. Garbinski, S. Luryi, D. L. Sivco, and A. Y. Cho, Phys. Rev. Lett. **67**, 2231 (1991).
[12] A. C. Morteani, P. Sreearunothai, L. M. Herz, R. H. Friend, and C. Silva, Phys. Rev. Lett. **92**, 247402 (2004).
[13] V. D. Mihailetchi, L. J. A. Koster, J. C. Hummelen, and P. W. M. Blom, Phys. Rev. Lett. **93**, 216601 (2004).
[14] J. Lehmann, S. Kohler, P. Hänggi, and A. Nitzan, Phys. Rev. Lett. **88**, 228305 (2002).
[15] J. Lehmann, S. Kohler, P. Hänggi, and A. Nitzan, J. Chem. Phys. **118**, 3283 (2003).
[16] S. Camalet, S. Kohler, and P. Hänggi, Phys. Rev. B **70**, 155326 (2004).
[17] S. Kohler, J. Lehmann, and P. Hänggi, Phys. Rep. **406**, 379 (2005).
[18] M. H. Pedersen and M. Büttiker, Phys. Rev. B **58**, 12993 (1998).
[19] M. Wagner and F. Sols, Phys. Rev. Lett. **83**, 4377 (1999).
[20] C. Caroli, R. Combescot, P. Nozieres, and D. Saint-James, J. Phys. C **4**, 916 (1971).
[21] Y. Meir and N. S. Wingreen, Phys. Rev. Lett. **68**, 2512 (1992).
[22] S. Datta, *Electronic Transport in Mesoscopic Systems* (North-Holland, Amsterdam, 1995).
[23] A.-P. Jauho, N. S. Wingreen, and Y. Meir, Phys. Rev. B **50**, 5528 (1994).
[24] H. M. Pastawski, Phys. Rev. B **46**, 4053 (1992).
[25] R. López, R. Aguado, G. Platero, and C. Tejedor, Phys. Rev. Lett. **81**, 4688 (1998).
[26] R. López, R. Aguado, G. Platero, and C. Tejedor, Phys. Rev. B **64**, 075319 (2001).
[27] R. López, D. Sánchez, and G. Platero, Phys. Rev. B **67**, 035330 (2003).
[28] R. Aguado, J. Iñarrea, and G. Platero, Phys. Rev. B **53**, 10030 (1996).
[29] A. P. Jauho and K. Johnsen, Phys. Rev. Lett. **76**, 4576 (1996).
[30] J. C. Cuevas, J. Heurich, A. Martin-Rodero, A. Levy Yeyati, and G. Schön, Phys. Rev. Lett. **88**, 157001 (2002).
[31] L. Arrachea, Phys. Rev. B **66**, 045315 (2002).
[32] L. Arrachea, Eur. Phys. J. B **36**, 253 (2003).
[33] L. Arrachea, Phys. Rev. B **70**, 155407 (2004).
[34] L. Arrachea and L. Cugliandolo, Europhys. Lett. **70**, 642 (2005).
[35] J. Rammer and H. Smith, Rev. Mod. Phys. **58**, 323 (1986).